USGS Award Number 06HQGR0058

LIQUEFACTION POTENTIAL MAP OF CHARLESTON, SOUTH CAROLINA BASED ON THE 1886 EARTHQUAKE

Final Report to the
United States Geological Survey

By:

Hossein Hayati and Ronald D. Andrus

Department of Civil Engineering
Clemson University
Lowry Hall, Box 340911
Clemson, South Carolina 29634-0911 USA
Telephone: (864) 656-0488
Fax: (864) 656-2670
E-mail: randrus@clemson.edu

February 2007

Research supported, in part, by the United States Geological Survey (USGS), Department of the Interior, under USGS award number 06HQGR0058. The views and conclusions contained in this document are those of the authors and should not be interpreted as necessarily representing the official policies, either expressed or implied, of the United States Government.

USGS Award Number 06HQGR0058

LIQUEFACTION POTENTIAL MAP OF CHARLESTON, SOUTH CAROLINA BASED ON THE 1886 EARTHQUAKE

Final Report to the United States Geological Survey by
Hossein Hayati[1], and Ronald D. Andrus[2]

Department of Civil Engineering
Clemson University
Lowry Hall, Box 340911
Clemson, South Carolina 29634-0911 USA
Telephone: (864) 656-0488
Fax: (864) 656-2670
E-mail: randrus@clemson.edu

ABSTRACT

A new liquefaction potential map of the peninsula of Charleston, South Carolina, is presented in this paper. Liquefaction potential is expressed in terms of the liquefaction potential index (LPI) developed by Iwasaki et al. and calculated using 44 cone penetration test profiles. The cone profiles are supplemented with information from the 1:24,000 scale geologic map by Weems and Lemon, as well as several first-hand accounts of liquefaction and ground deformation that occurred during the 1886 Charleston earthquake. Nearly all of the cases of liquefaction and ground deformation occurred in the Holocene to late Pleistocene beach deposits that flank the higher-ground sediments of the Wando Formation. To match the observed field behavior, an age correction factor of 1.8 is applied to the cyclic resistance ratios calculated for the 100,000-year-old Wando Formation. No age correction is needed for the younger deposits. The map can be a useful tool for planners, engineers, and scientists working to mitigate future earthquake damage in Charleston.

[1] Graduate Research Assistant, Dept. of Civil Engineering, Clemson Univ., Clemson, SC 29634-0911.
[2] Associate Professor, Dept. of Civil Engineering, Clemson Univ., Clemson, SC 29634-0911.

ACKNOWLEDGEMENTS

This research was supported, in part, by the United States Geological Survey (USGS), Department of the Interior, under grant number 06HQGR0058, with Ronald D. Andrus as Principal Investigator. The original project title of this grant is "Liquefaction Potential Mapping of the Charleston Quadrangle, South Carolina." The support of the USGS is greatly appreciated.

The authors also thank the many individuals who assisted with data collection, in particular, William M. Camp and Timothy J. Cleary of S&ME; Thomas J. Casey and William B. Wright of WPC; and Cedric D. Fairbanks, Nisha P. Mohanan and Aniket Shrikhande graduate students at Clemson University. Scott Brame and Janice Comfort of Clemson provided training in GIS and assistance with the search for first-hand earthquake accounts, respectively.

TABLE OF CONTENTS

INTRODUCTION

The Charleston, South Carolina earthquake of 1886 is the largest and most destructive historic seismic event to have occurred in the southeastern United States (Bollinger 1977). It caused 124 deaths and more than $460 million (2006 dollars) in damage (Côté 2006). Recent estimates of earthquake moment magnitude (M_w) for the event range from 6.9 $\pm$ 0.3 (Bakun and Hopper 2004) to 7.3 $\pm$ 0.3 (Frankel et al. 2002). Wong et al. (2005) estimated that a future repeat of the 1886 earthquake could cause as many as 900 deaths, more than 44,000 injuries, and a total economic loss of as much as $20 billion in South Carolina alone.

Presented in Figure 1 is the map of 1886 earthquake effects in the epicentral region by Bollinger (1977). The mapped damage, which is based on the Dutton (1889) report, includes numerous liquefaction craterlet areas and several locations of marked horizontal ground displacement. The liquefaction craterlets were as wide as 6.4 m. Although not shown on the map, liquefaction and horizontal ground displacements also occurred at several locations in the city of Charleston.

The geologic map of the city of Charleston by Weems et al. (1997) is shown in Figure 2. As illustrated in the map, the city of Charleston is bounded on the east by the Cooper River and on the west the Ashley River. During the past 300 years, much of the low-lying tidal marsh areas adjacent to the rivers (designated as Qht) have been built up with artificial fill (af) to allow the city to be constructed to the water's edge. On Drum Island, the extensive area of af is due to the heaping of spoils during periodic dredging of the harbor area (Weems and Lemon 1993). The natural higher ground making up the peninsula consists of two units of Pleistocene age sediments. The older Pleistocene unit (Qws) is the barrier-island facie of the Wando Formation. The younger Pleistocene unit (Qhes) is the beach deposits that flank the Wando Formation.

Elton and Hadj-Hamou (1990) developed the first liquefaction potential map of the Charleston peninsula using standard penetration test (SPT) borings. Their map, which is for a 50-year exposure time, indicates that much of the peninsula has more than a 20 % chance of liquefying. Recent studies by Balon and Andrus (2006) and Li and Juang (2006) using cone penetration test (CPT) soundings have also predicted a high potential for liquefaction. While these studies provide a general indication of the liquefaction potential, careful consideration of available geologic information and first-hand accounts of 1886 ground behavior that are dispersed in several reports have led to a greatly improved liquefaction potential map.

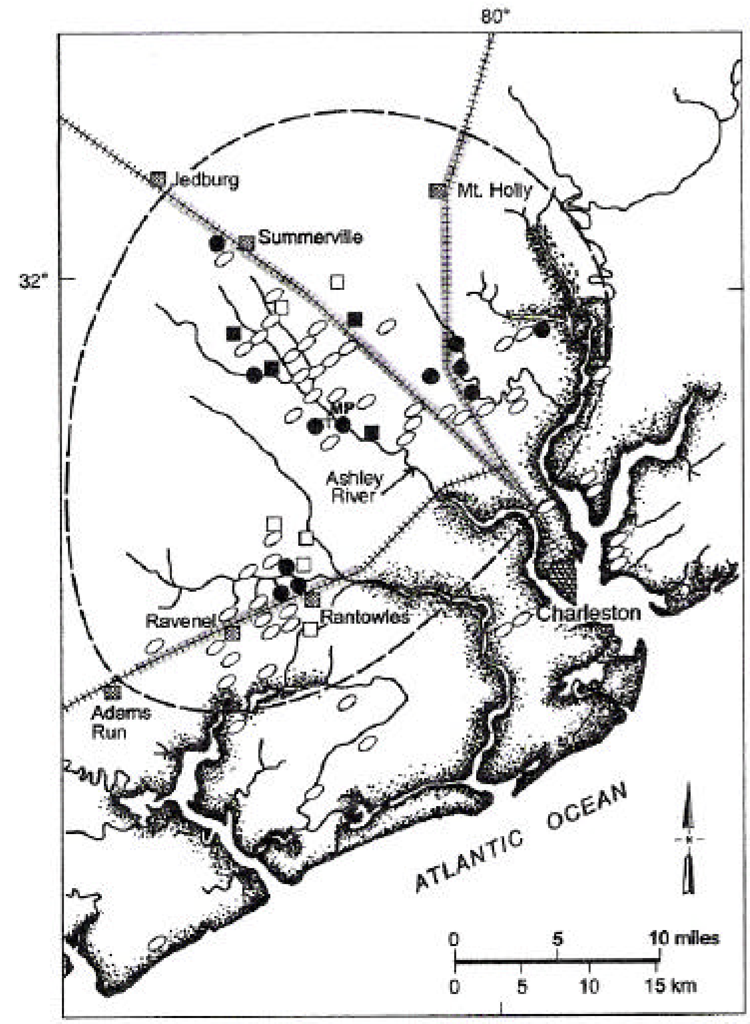

Explanation

ǂǂǂǂǂǂǂǂ	Railroad track damaged	⬭	Craterlet area
■	Building destroyed	□	Chimney destroyed
●	Marked horizontal displacement		

Figure 1. Map of 1886 earthquake effects near Charleston by Bollinger (1977).

This paper presents for the first time a detailed summary of reported 1886 liquefaction and ground deformation features on the Charleston peninsula. Also presented is an evaluation of liquefaction potential based on 44 CPTs. Liquefaction potential is expressed in terms of the liquefaction potential index (*LPI*) developed by Iwasaki et al. (1978, 1982). The *LPI* values are combined with available geologic information and field observations to develop the new liquefaction potential map of the peninsula.

1886 LIQUEFACTION AND GROUND DEFORMATION

Much of what is known of the occurrence of liquefaction and ground deformation during the 1886 earthquake is based on the first-hand observations of Mr. W. J. McGee, Mr. Earle Sloan, Dr. G. E. Manigault and others. Many of their observations are summarized in the reports by Dutton (1889). Robinson and Talwani (1983) reviewed Dutton (1889) and found 6 cases of liquefaction on the peninsula. Since 1983, many of the original notes and research materials on the earthquake were rediscovered and published in the report by Peters and Herrmann (1986). Based on a careful review of the rediscovered notes and materials, as well as newspaper reports and other sources, 27 cases of liquefaction and permanent ground deformation in the city of Charleston have been identified as part of this study.

Plotted in Figure 2 are the locations of the 27 cases of liquefaction and ground deformation. The cases have been grouped into three general categories—1) locations where sand and water were ejected out of the ground, 2) locations where fissures and/or permanent lateral ground displacement occurred without ejected sand and water, and 3) locations where settlement occurred without ejected sand and water. A detailed summary of the 27 cases is presented in Table 1.

Nearly all of the 12 cases of ejected sand and water plot in or immediately adjacent to the surficial geologic unit designated as Qhes (see Figure 2). The one exception being case 13, which plots in the surficial unit af where materials of Qhes and Qht could be interfingering. The liquefaction features range from small to large sand boils (cases 6, 11, 12, 13, 16, 19, 21, 24) to large volumes of material filling cellars (case 7) to columns of material being ejected from wells up to a height of 3-6 m (cases 4, 8, 17). In addition to these 12 cases, the News & Courier (1886, Sept. 7, p. 2) reports that "quite a number of cellars in all parts of the city were unaccountably filled with water where there had never been any water before."

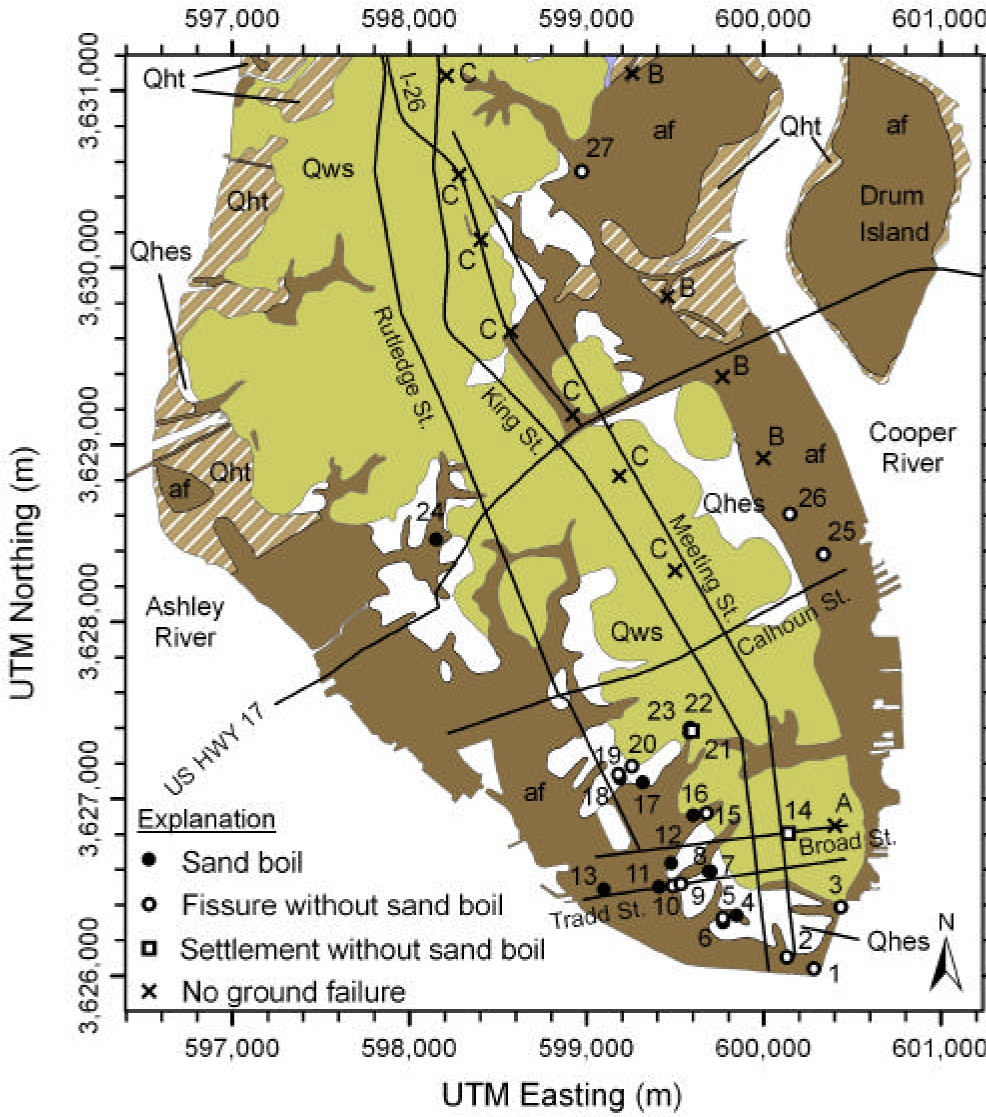

Figure 2. Geologic map of Charleston peninsula and Drum Island by Weems et al. (1997) showing locations of liquefaction and ground deformation in 1886.

Table 1. Cases of liquefaction and permanent ground deformation in the city of Charleston.

Location	Site Number and Description	Source
Battery	1 Heavy masonry of the battery displaced, opening cemented seams sometimes as much as 25-50 mm	Peters and Herrmann (1986, p. 35)
South Battery and King Streets—White Point Gardens	2 Curbstone around statue displaced and adjacent ground somewhat fissured	Peters and Herrmann (1986, p. 34)
Water and East Battery Streets—Mr. E. L. Wells residence	3 Fissures as wide as 25 mm trending parallel to Water Street	Peters and Herrmann (1986, p. 101-103)
Gibbes and Legare Streets—Mr. Hasel Heyward residence	4 Large volume of water and sand ejected from well in yard	News & Courier (Sept. 4, 1886, p. 1)
#6 Gibbes Street—Dr. G. E. Manigault residence	5 Fissures as wide as 20 mm trending north-south 6 Mud/sand spout with diameter of 0.9 m in yard of opposite house	Dutton (1889, p. 240-241); Peters and Herrmann (1986, p. 95)
#5 Logan Street—Mr. J. K. Blackman residence	7 Large volume of sand and water ejected from under main brick pillar and into cellar; pillar twisted 130 mm out of line 8 Large volume of sand and water ejected from fire well to a height of 3 m, and through pavement	Year Book (1886, p. 409-413); Dutton (1889, p. 266-268)
Council Street, 2nd building south of Tradd on east side	9 Wooden house moved 220 mm to south, north wall displaced as much as 250 mm 10 Row of houses immediately to east moved 50 mm to north	Peters and Herrmann (1986, p. 6, 15-17)
#167 Tradd Street	11 Fissure 150 mm wide with ejected sand and water trending parallel to Tradd Street	Peters and Herrmann (1986, p. 6, 15, 17)
Middle of Savage Street, on south-east side	12 Craterlets with ejected water and small quantity of sand, sod 75 mm diameter thrown 1.2-1.5 m	Peters and Herrmann (1986, p. 6, 17)
Tradd Street (west end)—Mr. Robert G. Chisolm residence	13 Fissures with ejected sand and water	Stockton (1986, p. 24-25)
Broad and Meeting Streets—St. Michaels Church	14 Tower footing settled unevenly about 200 mm; footing embedded to depth of 2.4-3 m and founded on a clay stratum 1.5-1.8 m thick; settlement may have been "caused by the near presence of the large Meeting street tidal drains"	Year Book (1886, p. 416); Peters and Herrmann (1986, p. 93-94); News & Courier (Sept. 7, 1886, p. 2)

Table 1. Cases of liquefaction and permanent ground deformation in the city of Charleston. (Continued.)

Location	Site Number and Description	Source
Queen and Mazych Streets (southeast corner)	15 North wall thrown out and extremely cracked; west wall scarcely cracked	Peters and Herrmann (1986, p. 7, 17)
#139 Queen Street—residence of Lieut. Goulden	16 Fissure parallel to street with ejected sand and water	Peters and Herrmann (1986, p. 6, 17)
Beaufain Street	17 Water and mud ejected from wells along street reaching a height of 4.5 m or 6 m	News & Courier (Sept. 4, 1886, p. 1)
#157 Wentworth Street—Mr. Frank R. Fisher residence	18 Fissures trending northeast on higher ground; front wall of house bulged outward 19 Fissures trending southeast with ejected water and sand on lower ground	Dutton (1889, p. 242-247)
#149 Wentworth Street—Mr. Francis S. Rodgers residence	20 Fissures split the west end of the house	Dutton (1889, p. 246); Stockton (1986, p. 45)
#104 Wentworth Street—Mr. S. G. Pinckney residence	21 Large volume of sand and water ejected from fissure in yard	News & Courier (Sept. 7, 1886, p. 2)
#100 Wentworth Street—Grace Episcopal Church	22 Tower settled up to 115 mm 23 Brick columns supporting structure 220 mm out of plumb, with southward ground movement	Stockton (1986, p. 77-78)
Line Street	24 "Water around Line Street is said to have been boiling"	News & Courier (1886, Sept. 1, p. 8)
Charlotte and Washington Streets (southeast corner)—Gas Works	25 Vacant space between brick lining of large circular wall (diameter of 39 m to depth of 7.6 m) with width of about 200 mm on the southeast side; on northwest side, vacant space with width of 50 mm	Year Book (1886, p. 392-393); Dutton (1889, p. 237, 255-256); Peters and Herrmann (1986, p. 50, 92-93)
Common track of the Charleston & Savannah Rail Road, and North Eastern Rail Road, near station	26 Near station—Cylindrical masonry wall enclosing turntable strained to southeast 27 2.4 km (1 mile + 2500 ft) from station—Flexure to east expressed in curve with 0.46 m ordinate to 914 m chord	Peters and Herrmann (1986, p. 52)

The 13 cases of fissures and/or horizontal ground displacement without ejected sand and water also plot in or immediately adjacent to the surficial geologic unit Qhes (see Figure 2). These cases can be roughly divided by the amount of lateral ground movement—less than about 50 mm (cases 1, 2, 26), 50 mm to 200 mm (cases 3, 5, 10, 15, 18, 20, 25), and over 200 mm (cases 9, 23, 27). They indicate that lateral spreading occurred at many locations in Qhes.

Lateral spreading is one of four basic types of liquefaction-induced ground failure (National Research Council 1985). The other three types are flow failure, ground oscillation, and loss of bearing capacity. Flow failures occur in areas where ground slope is $\geq$ 5 %, and have lateral movements on the order of tens of meters. Lateral spreads occur in areas of 0.5-5 % ground slope, and have lateral movements of a few meters or less. Ground oscillations occur where the ground surface is too flat to permit lateral movement (< 0.5 %). Because much of the Charleston peninsula has ground surface slopes less than 5 %, lateral spreading, ground oscillation, and loss of bearing capacity are the expected types of liquefaction-induced ground failure.

There are several first-hand observations that indicate ground oscillation also occurred in the Qhes deposits on the west side of the peninsula. Perhaps the most vivid account is that of Dr. Franis L. Parker, a surgeon who was walking on Tradd Street between Logan and Greenhill Streets at the time of the earthquake (between cases 7, 8, 9 and 10 in Figure 2). The following is Dr. Paker's account (Dutton 1889, p. 265-268):

> "The waves seemed then to come from both the southwest and northwest and crossed the street diagonally, intersecting each other, and lifting me up and letting me down as if I were standing on a chop sea. I could see perfectly and made careful observation, and I estimate that the waves were at least two feet [0.6 m] in height."

Mr. J. K. Blackman, at his home on Logan Street (cases 7 and 8), described the motion as "conflicting." Capt. F. W. Dawson, at his home on Bull Street near Rutledge, described the motion "like a ship at sea" (Year Book 1886, p. 413).

The two cases where settlement occurred without ejected sand and water (based on the first-hand accounts reviewed by the authors) involve the towers at St. Michaels Church (case 14) and Grace Episcopal Church (case 23). Grace Episcopal Church is located just in artificial fill (af) where Qhes is believed to be present in the subsurface. On the other hand, St. Michaels Church represents the only case of ground deformation located in Qws. A News & Courier

(1886, Sept. 7, p. 2) article suggested that the heavy damage~~s~~ sustained by St. Michael's Church might have been caused by the near presence of the large Meeting Street tidal drains. It was speculated in the newspaper article that a "very slight slide say of half an inch [13 mm] would be sufficient to produce the present condition." Thus, it may not be appropriate to attribute the settlement of St. Michaels Church tower to liquefaction-induced ground deformation.

The abundant cases of fissures and ejected sand and water indicate that the liquefaction potential was moderate to high in Qhes. On the other hand, the few cases of ground deformation in Qht and Qws suggest that the liquefaction potential was low to moderate in these deposits. Additional evidence supporting the low liquefaction potential for Qws and Qht deposits are the detailed earthquake observations that did not mention any ground deformation. These cases are summarized in Table 2. They include the account of a news editorial staff outside the News & Courier building (case A). They also include the detailed field notes of Mr. Earle Sloan (Peters and Herrmann 1986) of train tracks leaving the city where displacements were inappreciable (cases B and C). These cases of no surface manifestations of liquefaction provide further support for low to moderate liquefaction potential in Qws and Qht deposits.

CPT DATABASE

Locations of 78 CPT sites are plotted on the geologic map of Charleston peninsula shown in Figure 3. As summarized in Table 3, the CPTs were performed by four different organizations (i.e., ConeTec, Gregg In Situ, S&ME, and WPC). The letter(s) beginning each site code given in the table indicates the performing organization. The first two numbers following the letter(s) indicate the year the test was performed. The remaining numbers and letters indicate the specific project number and test location. For example, the CPT at site number 1 with site code of W01194-CPT1 was performed by WPC in 2001 for project number 194 at test site CPT1. Latitudes and longitudes were given in the project reports for many of the test sites. For sites where latitudes and longitudes were not given, they are approximated using project site address information and the GoogleEarth (http://earth.google.com) free software. Location accuracy is believed to be within 100 m.

Table 2. Cases of no surface manifestations of liquefaction in the city of Charleston.

Location	Site Number and Description		Source
#19 Broad Street—The News and Courier building	A	No mention of any surface manifestations of liquefaction in detail observations outside building by news editorial staff	Year Book (1886, p. 351-353)
Common track of Charleston & Savannah Rail Road, and North Eastern Rail Road lines, 0-1.6 km (0-1 miles)	B	"Displacement inappreciable"; "alternate embankments & trusses crossing extensive marsh tract bordering city on north"	Peters and Herrmann (1986, p. 52)
South Carolina Rail Road line, 0-4.8 km (0-3 miles)	C	No ground displacement or other surface manifestations of liquefaction recorded	Peters and Herrmann (1986, p. 54)

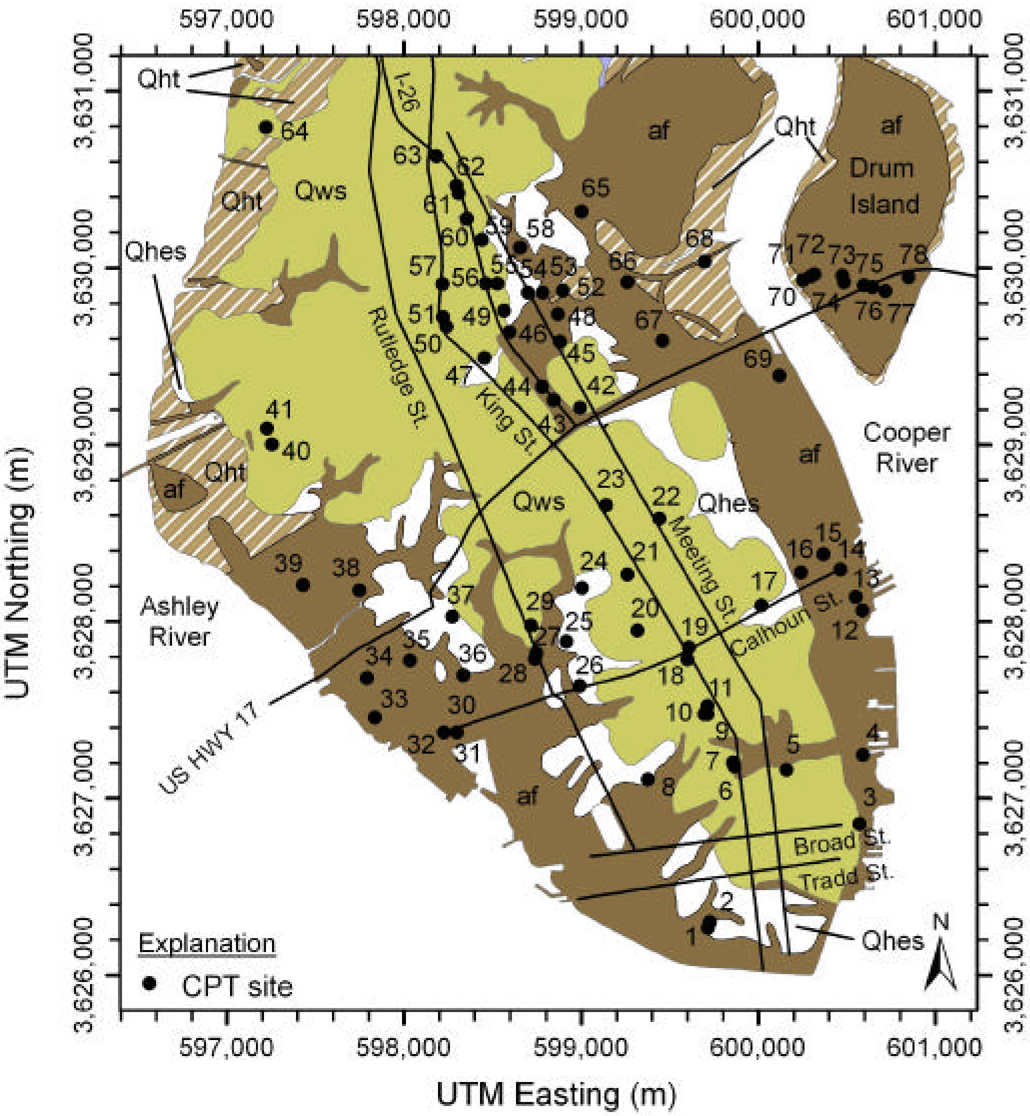

Figure 3. Geologic map of Charleston peninsula and Drum Island by Weems et al. (1997) showing locations of CPT sites.

Table 3. Summary of CPT soundings from Charleston peninsula and Drum Island

Site number	Site code[a]	Latitude (degree)	Longitude (degree)	Electronic file available?	Maximum test depth (m)	Water table depth (m)	Top of Cooper Marl depth (m)	Top of Wando Formation depth (m)	Inferred geology in top 10 m	Site geology category
1	W01194-CPT1	32.7715	-79.9353	Yes	24.3	1.2	23.1?[b]	9.1	Qhes/Qws	Qhes
2	W01194-CPT2	32.7718	-79.9352	Yes	10.4	1.2	23.1?	8.8	Qhes/Qws	Qhes
3	W03106-SC1	32.7767	-79.9261	Yes	14.3	1.7	15.2?	4.3	af/Qhes/Qws	Qhes
4	S04015-C1	32.7802	-79.9259	No	21.3	0.9	17.1	14.0?	af/Qht	Qht
5	S05332-CPT1	32.7795	-79.9305	No	18.3	1.8	16.2	0.0	Qws/Qwc	Qws
6	W00363-CPT2	32.7797	-79.9336	Yes	15.8	2.3	17.9?	1.2	af/Qws/Qwc	Qws
7	W00363-SCPT1	32.7799	-79.9337	Yes	18.9	2.3	17.9	1.5	af/Qws	Qws
8	W04321-C1	32.7791	-79.9388	No	24.1	0.8	23.2?	7.6	af/Qhes/Qhec/Qws	Qhes
9	S02457-B2	32.7824	-79.9352	Yes	21.6	1.8	>21.3	0.0	Qws/Qwc	Qws
10	S04262-C1	32.7824	-79.9354	No	26.8	2.1	21.9	0.0	Qws/Qwc	Qws
11	S02457-B1	32.7828	-79.9352	Yes	25.3	1.4	22.5	0.0	Qws/Qwc	Qws
12	GRG2-CPT2	32.7876	-79.9258	No	17.3	3.7	18.2	14.6	af/Qht	Qht
13	S02105-B2	32.7883	-79.9262	Yes	22.8	1.2	18.2	18.2?	af/Qht	Qht
14	W99175-SCPT1	32.7897	-79.9271	Yes	37.8	1.0	24.6	18.2?	af/Qht	Qht
15	S04902-CPT1	32.7905	-79.9281	No	26.7	1.5?	25.0	17.1?	af/Qht	Qht
16	S04952-B1	32.7896	-79.9295	No	23.7	1.5	23.3	13.4?	af/Qht	Qht
17	W02054-C1	32.7879	-79.9319	Yes	27.1	1.1	27.1	5.2?	Qhes/Qhec	Qhes
18	S01402-S1	32.7852	-79.9364	Yes	24.3	1.8	21.0	0.0	Qws/Qwc	Qws
19	S03462-S1	32.7858	-79.9363	Yes	30.4	0.9	28.3	0.0	Qws	Qws
20	S01355-B-2A	32.7867	-79.9394	Yes	25.9	2.4	23.7	0.0	Qws/Qwc	Qws
21	W04470-CPT1	32.7896	-79.9400	No	20.1	1.7	17.2	0.0	Qws/Qwc	Qws
22	W04030-SC1	32.7924	-79.9380	Yes	19.8	2.5	17.1	0.0	Qws/Qwc	Qws
23	S01033-CPT1	32.7931	-79.9412	Yes	16.4	1.8	16.4	0.0	Qws/Qwc	Qws
24	W02288-SC2	32.7889	-79.9427	Yes	16.7	2.3	15.5	8.5?	Qhes/Qhec/Qws	Qhes
25	S03593-CPT1	32.7862	-79.9437	No	22.9	0.4	21.3	7.3	Qhes/Qhec	Qhes
26	S02578-B1	32.7839	-79.9429	Yes	20.4	1.5	21.9	9.1	Qhes/Qhec/Qws	Qhes
27	W03114-SC2	32.7856	-79.9455	Yes	25.3	1.6	24.3	8.2	af/Qht/Qws	Qht/Qhes

Table 3. Summary of CPT soundings from Charleston peninsula and Drum Island (Continued)

Site number	Site code[a]	Latitude (degree)	Longitude (degree)	Electronic file available?	Maximum test depth (m)	Water table depth (m)	Top of Cooper Marl depth (m)	Top of Wando Formation depth (m)	Inferred geology in top 10 m	Site geology category
28	S02354-B4	32.7853	-79.9456	Yes	30.4	1.2	25.2	8.5	af/Qht/Qhec/Qws	Qht/Qhes
29	S03590-C1	32.7870	-79.9458	No	24.0	0.8	23.2	0.0	Qws/Qwc	Qws
30	S01369-A5	32.7816	-79.9503	Yes	24.3	3.1	17.9	17.9?	af/Qht/Qhes	Qht/Qhes
31	S01369-B2	32.7816	-79.9503	Yes	24.3	3.1	17.6	17.6?	af/Qht/Qhes	Qht/Qhes
32	W04312-C1	32.7816	-79.9511	No	20.1	0.5	15.5?	12.2?	af/Qht	Qht
33	W04355-SC1	32.7824	-79.9553	No	18.7	0.9	18.6?	14.9?	af/Qht	Qht
34	W01352-SC1	32.7844	-79.9557	Yes	20.7	1.1	18.9	12.8	af/Qht	Qht
35	W01082-CPT1	32.7853	-79.9531	Yes	19.8	0.6	18.7	12.5	af/Qht	Qht
36	S00219-B1	32.7845	-79.9499	Yes	27.4	1.2?	18.2	13.7?	af/Qht	Qht
37	S041060-C2	32.7875	-79.9505	No	22.0	0.9	19.2	5.8	Qhes/Qhec/Qws	Qhes
38	S01357-B2	32.7889	-79.9561	Yes	21.3	1.1	13.4	11.3	af/Qht	Qht
39	S01420-S1	32.7892	-79.9595	Yes	22.5	0.9?	13.7	11.3	af/Qht	Qht
40	S01317-B2	32.7964	-79.9613	Yes	22.8	2.1	15.2	0.0	Qws/Qwc	Qws
41	S01317-B1	32.7972	-79.9616	Yes	13.7	2.1	14.6?	0.0	Qws/Qwc	Qws
42	C98706-C12	32.7981	-79.9427	No	42.6	2.1	18.5	0.0	Qws/Qwc	Qws
43	S99876-CHS20	32.7985	-79.9443	Yes	40.0	2.3	19.8	1.2	af/Qws/Qwc	Qws
44	C98706-C11	32.7992	-79.9450	No	54.9	NA[c]	19.8	5.2?	af/Qws	Qws
45	S01627-S1	32.8015	-79.9439	Yes	27.3	1.2	18.7	11.6	af/Qhes/Qhec	Qhes
46	C98706-C9	32.8020	-79.9469	No	42.8	NA	17.4	3.0?	af/Qws/Qwc	Qws
47	S04894-C1	32.8007	-79.9484	No	21.3	0.6	16.2	5.5?	Qal?/Qws	Qws
48	S99876-CHS26	32.8029	-79.9440	Yes	38.7	0.6	16.7	16.7?	af/Qht	Qht
49	C98706-C7	32.8031	-79.9472	No	54.9	NA	17.4	0.0	Qws/Qwc	Qws
50	S00217-B4	32.8023	-79.9507	Yes	21.3	1.5	19.2	0.0	Qws/Qwc	Qws
51	W01059-CPT2	32.8028	-79.9509	Yes	15.8	1.7	15.8?	0.0	Qws/Qwc	Qws
52	C98706-C13	32.8041	-79.9437	No	42.8	NA	17.1	11.6?	Qht	Qht
53	S99876-CHS24	32.8040	-79.9449	Yes	45.7	0.9	18.5	5.5	af/Qhes/Qws/Qwc	Qhes
54	C98706-C8	32.8040	-79.9458	No	42.6	0.9	16.4	6.4	Qhes/Qhec/Qws	Qhes

Table 3. Summary of CPT soundings from Charleston peninsula and Drum Island (Continued)

Site number	Site code[a]	Latitude (degree)	Longitude (degree)	Electronic file available?	Maximum test depth (m)	Water table depth (m)	Top of Cooper Marl depth (m)	Top of Wando Formation depth (m)	Inferred geology in top 10 m	Site geology category
55	C98706-C6	32.8045	-79.9476	No	42.8	NA	19.8	0.0	Qws/Qwc	Qws
56	C98706-C5	32.8045	-79.9483	No	42.8	NA	17.4	0.0	Qws/Qwc	Qws
57	W02100-SCPT1	32.8045	-79.9509	Yes	18.9	2.5	17.0	0.0	Qws/Qwc	Qws
58	C98706-C10	32.8063	-79.9462	No	42.6	1.7	19.2	7.0	af/Qht/Qws	Qht/Qhes
59	C98706-C4	32.8067	-79.9485	No	42.6	2.5	21.6	0.0	Qws	Qws
60	C98706-C3	32.8078	-79.9494	No	42.8	NA	19.8	0.0	Qws/Qwc	Qws
61	S99876-CHS4	32.8091	-79.9499	Yes	39.2	1.5	16.7	0.0	Qws	Qws
62	C98706-C2	32.8095	-79.9500	No	54.9	NA	17.1	0.0	Qws	Qws
63	C98706-C1	32.8110	-79.9512	No	42.8	NA	20.7	0.0	Qws	Qws
64	S02629-CPT1	32.8126	-79.9615	No	14.8	2.6	14.0?	0.0	Qws/Qwc	Qws
65	W01343-SCPT1	32.8081	-79.9425	Yes	21.9	2.7	19.8	7.9	af/Qht/Qws	Qht/Qhes
66	C98706-C15	32.8045	-79.9398	No	54.9	1.4	18.9	10.0	af/Qht	Qht
67	W02092-SCPT1	32.8015	-79.9377	Yes	18.9	1.5	15.2	10.6	af/Qht	Qht
68	C98706-C17	32.8055	-79.9351	No	42.8	NA	22.3	21.6	af/Qht	Qht
69	S01071-B1	32.7997	-79.9307	Yes	18.3	1.1	17.2	17.2	af/Qht	Qht
70	S99876-ML15	32.8045	-79.9292	Yes	16.5	0.6	16.1	15.2	af/Qht	Qht
71	C98706-C20	32.8047	-79.9287	No	54.0	NA	25.0?	21.9?	af/Qht	Qht
72	S99876-ML16	32.8048	-79.9285	Yes	21.3	3.5	22.5	20.4	af/Qht	Qht
73	C98706-C21	32.8047	-79.9268	No	42.6	2.5	22.2	20.4	af/Qht	Qht
74	S99876-ML18	32.8044	-79.9267	Yes	21.3	5.3	22.5	21.3	af/Qht	Qht
75	S99876-ML22	32.8042	-79.9255	Yes	26.4	0.2	13.7	11.6	af/Qht	Qht
76	C98706-C22	32.8041	-79.9250	No	53.9	NA	20.1?	15.5	af/Qht	Qht
77	S99876-ML24	32.8039	-79.9242	Yes	48.4	0.6	16.1	15.2	af/Qht	Qht
78	C98706-C23	32.8046	-79.9228	No	42.6	0.5	15.5	15.2	af/Qht	Qht

[a] C = ConeTec; GRG = Gregg In Situ, Inc.; S = S&ME, Inc; W = WPC, Inc.
[b]? = Some uncertainty in exact value. Value listed is a conservative estimate.
[c]NA = Not available.

Electronic files are available for 44 of the 78 CPTs (Fairbanks et al. 2004; Mohanan 2006). Of the 44 CPTs, 30 extend to depths more than 20 m, the maximum depth required for *LPI* calculations. The other 14 CPTs either extend into the Tertiary-age Cooper Group or to within 2 m of the Cooper Group based on the elevation contour map by Fairbanks (2006). The one exception to this is CPT number 2, which extends to a depth of just 10.4 m. For this site, the portion of the adjacent CPT (i.e., number 1) profile between 10.4 m and 20 m is assumed. For the 3 soundings that reach within 2 m of the Cooper Group (i.e., sites numbers 3, 6, 41), the missing portion of the profile above the Cooper is assumed to be the same as in the last 2 m of the measured profile. These criteria and assumptions are adopted to maximize the number of electronic files available for analysis, yet minimize errors in the *LPI* calculations. Although only hard copies of the profiles are available for the other 34 CPT soundings, they are also useful in interpreting the geology beneath the peninsula.

The Cooper Group, locally known as the Cooper Marl, is a well-compacted, sometimes partially lithified calcarenite that classifies as silty clay to clayey silt. It is generally assumed to be non-susceptible to liquefaction (Li et al. 2007). In seismic CPT profiles, the Cooper Marl is characterized by fairly uniform tip resistances, pore pressure measurements made with the transducer located immediately behind the cone tip (in the u_2 position) that typically exceed 10 MPa, and shear-wave velocity (V_s) values on the order of 400 m/s (Andrus et al. 2006).

The dominant geology in the top 10 m listed in Table 3 is inferred from the geologic map by Weems and Lemon (1993) and the CPT profiles. Near-surface geologic units include: man-made (or artificial) sand to clayey sand fills of diverse origin less than 300 years old (af); Holocene tidal marsh clayey sand to clay deposits less than 5,000 years (Qht); Holocene alluvial sand deposits along some drainage courses (Qal) with age less than 10,000 years; early Holocene to late Pleistocene estuarine silt to clay deposits with age ranging from 6,000 to 85,000 years (Qhec); late Pleistocene beach to barrier-island sand deposits ranging in age from 33,000 to 85,000 years (Qhes); and various facies of the Wando Formation ranging from 70,000 to 130,000 years, including barrier-island sands (Qws) and estuarine to fluvial clays (Qwc).

Representative CPT, V_S, and geologic profiles are presented in Figure 4. These profiles are from CPT site number 26 (see in Figure 3). CPT tip resistances are corrected to account for the effect of water pressure acting behind the cone tip (q_t). The friction ratio (*FR*) is defined as the cone sleeve resistance measurement divided by q_t. Values of *FR* are usually much greater (over 1 %) in clayey soils than sandy soils. Hydrostatic pore pressures (u_0) are assumed equal to the depth below the groundwater table multiplied by the unit weight of water. Values of u_2 close to u_0 indicate freely draining soil (e.g., sand); and higher u_2 values indicate lower permeable soil (e.g., clay). Thus, the materials in Figure 4 at depths of 4.5-8.5 m and 11.4-15.0 m are clayey soils. Between 9 m and 11 m, the higher values of q_T, lower values of FR, and u_2 values near the hydrostatic line indicate sandy material. Values of V_s, ranging from about 100 m/s to nearly 400 m/s in the figure, are a measure of soil stiffness, with the lower values indicating soft or loose soil.

The geologic profile shown in Figure 4(e) consists of 9 m of Holocene to late Pleistocene deposits underlain by 10 m of the Wando Formation. Two distinguishing features between younger and older clay deposits are the u_2 and V_s values. Values of $(u_2\text{-}u_0)/\sigma'_v$ are typically less than 3 in Qht deposits and between 3 and 7 in Qws deposits. Values of V_s are, on average, 110 m/s in Qhes/Qhec and 190 m/s in Qws/Qwc (Andrus et al. 2006). The values V_s plotted in Figure 4(d) for the younger and older deposits are consistent with these average values.

PROCEDURE

The Liquefaction Potential Index (LPI) was developed by Iwasaki et al. (1978, 1982) for predicting the liquefaction severity at a site through considering the soil profile in the top 20 m. It can be written in integral form as (Iwasaki et al. 1978):

$$LPI = \int_0^{20} Fw(z)dz \tag{1}$$

where F is a function of factor of safety against liquefaction (FS) defined as F = 1-FS for $FS \leq 1$ and F = 0 for FS >1, z is the depth in m, and $w(z)$ is a depth-weighting factor equal to 10-0.5z. In summation form, LPI can be expressed as:

$$LPI = \sum_{i=1}^{n} F_i w_i(z) H_i \tag{2}$$

where F_i is the function of FS of the i^{th} layer, $w_i(z)$ is the depth-weighting factor of the i^{th} layer, H_i is the thickness of the i^{th} layer in meters, and n is the number of layers in the top 20 m.

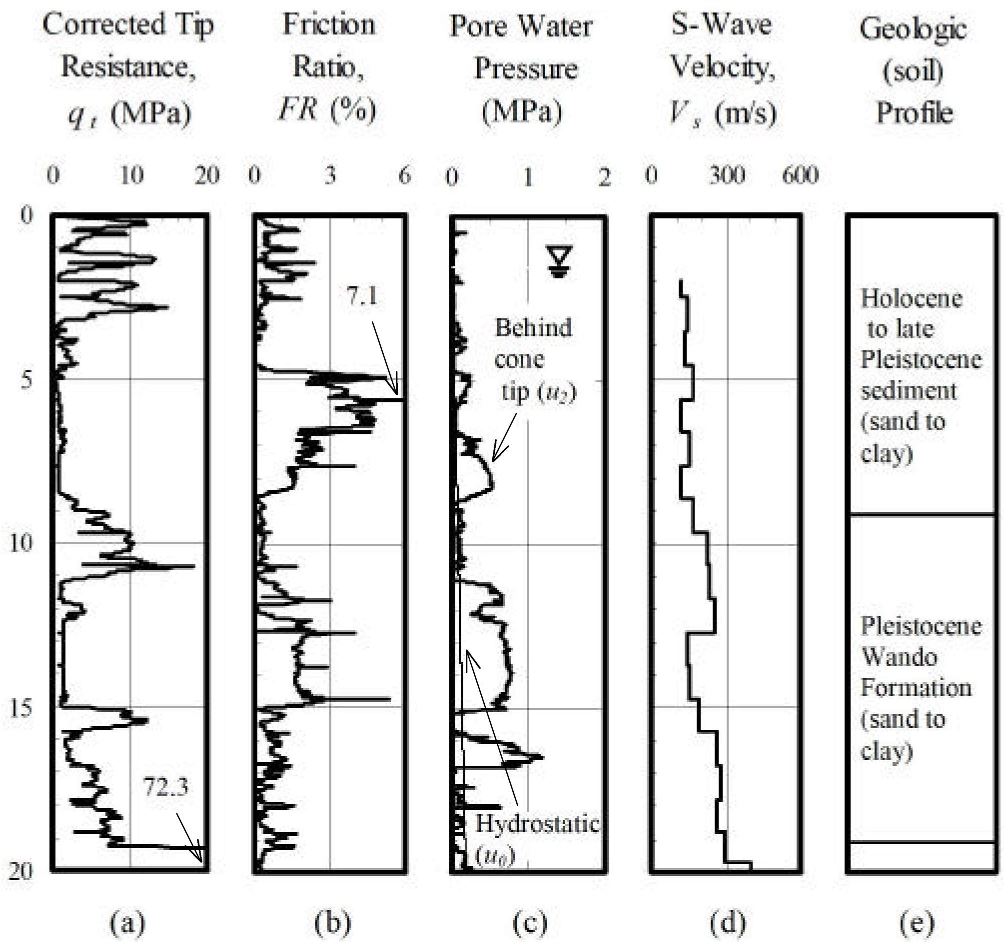

Figure 4. Representative cone tip q_t, *FR*, pore water pressure, V_s, and geologic profiles from CPT site number 26.

Equations 1 and 2 assume that the severity of liquefaction is proportional to the amount by which *FS* is less than 1.0, the thickness of the low *FS* layer, and the proximity of the low *FS* layer to the ground surface.

To calculate *FS*, Iwasaki et al. (1978, 1982) adopted the simplified procedure for evaluating liquefaction resistance originally proposed by Seed and Idriss (1971). In the Seed and Idriss (1971) simplified procedure, *FS* is defined as the cyclic resistance ratio divided by the cyclic stress ratio. Brief explanations of the cyclic stress ratio, the cyclic resistance ratio, the criteria for screening out non-liquefiable clayey soils, and the general *LPI* criteria are presented below.

Cyclic Stress Ratio

The cyclic stress ratio (*CSR*) represents the seismic demand or loading on the soil and can be expressed as (after Seed and Idriss 1971; Youd et al. 2001):

$$CSR = 0.65\left(\frac{s_v}{s'_v}\right)\left(\frac{a_{max}}{g}\right)(r_d)/(MSF \times K_s) \qquad (3)$$

where s_v is the vertical total stress in the soil at the depth considered, s'_v is the vertical effective stress, a_{max} is the peak ground surface acceleration in g, g is the acceleration of gravity, r_d is a depth-dependent shear stress reduction factor, *MSF* is a magnitude scaling factor that accounts for the effects of shaking duration, and K_s is an overburden correction factor.

For this study, the general procedure outlined in Youd et al. (2001) is followed to provide *LPI* values comparable with the U.S. Geological Survey hazard mapping work in California (e.g., Toprak and Holzer 2003; Holzer et al. 2006). Values of r_d are calculated using the relationship by Liao and Whitman (1986). Values of *MSF* are calculated using the lower bound formulation suggested in Youd et al. (2001), which can be expressed as $MSF = (M_w/7.5)^{-2.56}$. Values of K_s are calculated using the equation proposed by Hynes and Olson (1999), which is expressed as $K_s = (s'_v / P_a)^{(f-1)}$ where P_a is a reference pressures assumed to be atmospheric pressure (about 100 kPa) in the same units as s'_v, and f is a function of relative density. Relative densities are estimated from CPT tip resistance measurements using the expression given by Idriss and Boulanger (2003).

Cyclic Resistance Ratio

The cyclic resistance ratio (*CRR*) represents the capacity of the soil to resist liquefaction. The relationship recommended by Youd et al. (2001) for computing *CRR* from CPT measurements can be expressed as (Robertson and Wride 1998):

$$\text{If } (q_{c1N})_{cs} < 50 \qquad CRR = 0.833\left(\frac{(q_{c1N})_{cs}}{1000}\right) + 0.05 \tag{4a}$$

$$\text{If } 50 \leq (q_{c1N})_{cs} < 160 \qquad CRR = 93\left(\frac{(q_{c1N})_{cs}}{1000}\right)^3 + 0.08 \tag{4b}$$

where $(q_{c1N})_{cs}$ is the clean-sand cone tip resistance normalized to atmospheric pressure.

The stress-normalized cone tip resistance (q_{c1N}) is calculated using the following equation (Robertson and Wride 1998):

$$q_{c1N} = C_Q\left(\frac{q_c}{P_a}\right) = \left[\frac{P_a}{s'_v}\right]^n \left(\frac{q_c}{P_a}\right) \tag{5}$$

where q_c is the measured cone tip resistance in the same units as P_a, and n is an exponent that depends on soil type. To avoid unreasonably high values at shallow depths, Youd et al. (2001) recommended that C_Q be limited to a maximum value of 1.7. For cone measurements made with a pressure transducer behind the cone tip, values of q_c are corrected for the effect of pore pressures (Lunne et al. 1997). This correction is particularly significant in silty soils. The exponent n is a variable that depends on soil type and is assumed as 0.5 for granular soils and 1.0 for clay.

Several investigators have noted that liquefaction resistance of soils increases with age (e.g., Seed 1979; Youd and Hoose 1977; Youd and Perkins 1978; Arango et al. 2000; Leon et al. 2006). However, because the processes causing increased liquefaction resistance with age were poorly understood and proposed correction factors for age had not been verified, Youd et al. (2001) did not recommended age correction factors at the time of their study. In an effort to account for the affect of age on *CRR*, the following correction equation has been proposed (Andrus et al. 2004):

$$CRR_a = CRR \times K_{a2} \tag{6}$$

where CRR_a is the age-corrected cyclic resistance ratio, and K_{a2} is a factor to correct for influence of age. The value of K_{a2} is 1.0 for soils less than a few thousand years old. For older soils, Andrus et al. (2004) suggested using the lower bound of the relationship between cyclic strength and time proposed by Arango et al. (2000). In this study, Equation 6 and the *LPI* procedure are used to estimate likely values of K_{a2} for near-surface soils in Charleston.

Screening for Non-Liquefiable Clayey Soils

In general, soils that are too clay rich are considered not susceptible to liquefaction (e.g., Seed and Idriss 1982; Robertson and Wride 1998; Youd et al. 2001; Bray and Sancio 2006; Boulanger and Idriss 2006). Robertson and Wride (1998) suggested that soils with soil behavior type index I_c > 2.6 and normalized friction ratio F_N > 1 % are likely non-liquefiable. The variables I_c and F_N are defined by following equations (Lunne et al. 1997; Robertson and Wride 1998):

$$I_c = \left[(3.47 - log_{10}\, q_{c1N})^2 + (log_{10}\, F_N + 1.22)^2\right]^{0.5} \tag{7}$$

and

$$F_N = f_s / (q_c - s_v) \times 100\% \tag{8}$$

where f_s is the cone sleeve resistance.

In this study, the *LPI* value is obtained for each of the 44 CPT sites after first screening out any measurement interval above the Cooper Marl with I_c > 2.6. The cutoff of I_c = 2.6 based on Equation 7, above which soil is deemed too clay rich to liquefy, may be "too conservative" for some soils (Gilstrap 1998; Zhang et al. 2002; Li et al. 2007), meaning that a somewhat lower cutoff value might be more reasonable on average. However, without a better approach at this time, it is assumed that any layer above the Marl with I_c > 2.6 will not liquefy.

***LPI* Criteria**

LPI values calculated using Equations 1 and 2 theoretically could range from 0 to 100. The minimum value of 0 is obtained where *FS* > 1 over the entire 20 m depth. The maximum value of 100 is obtained where *FS* = 0 over the entire 20 m depth.

Based on performance of sites in six Japanese earthquakes and using the Seed-Idriss (1971) simplified procedure based on SPT blow count, Iwasaki et al. (1982) concluded that severe liquefaction is most likely to occur at sites where *LPI* > 15; and liquefaction is not likely to occur at sites where *LPI* < 5. For sites where *LPI* is between 5 and 15, moderate liquefaction is expected. Subsequent work by Toprak and Holzer (2003) using CPT measurements at sites shaken by the 1989 Loma Prieta, California earthquake provided results that agreed well with the *LPI* criteria proposed by Iwasaki et al. (1982). Thus, the *LPI* procedure of Iwasaki et al. (1982) is applied to the 44 CPT profiles with available electronic files.

LPI CALCULATIONS

The *LPI* calculations are first performed assuming M_w = 7.1 and a_{max} = 0.3 g, and without applying an age correction factor to *CRR* (i.e., K_{a2} = 1.0 for all geologic units). An M_w of 7.1 is the middle-range value of recent estimates mentioned earlier in this paper. An a_{max} of 0.3 g agrees well with the middle-range value based on ground motion studies by Elton and Marciano (1990), Silva et al. (2003) and Chapman et al. (2006) for the study area during the 1886 earthquake. The initial results are then compared with the observed field behavior presented previously to assess the need for any change in a_{max} or K_{a2}.

To simplify analysis of the results, the CPT sites are grouped in the last column of Table 3 into four site geology categories based on dominant geology in top 10 m—1) Qht, 2) Qht/Qhes, 3) Qhes, and 4) Qws. The first category comprises all sites where Qht extends to a depth of at least 10 m. This includes sites where Qht lies beneath af. The second category comprises sites where Qht is present but does not extend to a depth of 10 m. The third category comprises sites where Qhes is present at the ground surface or beneath af. There is no minimum depth (or thickness) requirement for Qhes to be included in the third category. Finally, the fourth category consists of all sites where Qws is present at the groundwater table. Of the 44 CPTs with available electronic files, there are 15, 5, 8 and 16 in the four site geology categories, respectively.

Without Age Correction

Presented in Figure 5 is an example of the *LPI* procedure applied to site number 26 (see Figure 3) assuming M_w = 7.1 and a_{max} = 0.3 g. Profiles of q_t and I_c versus depth are shown in Figure 5(a) and 5(b), respectively. Figure 5(c) depicts the calculated *CSR* and *CRR* values versus depth. The solid line represents the *CRR* values calculated without applying an age correction factor. Values of *FS* versus depth are presented in Figure 5(d). Figure 5(e) depicts the accumulated *LPI* with depth.

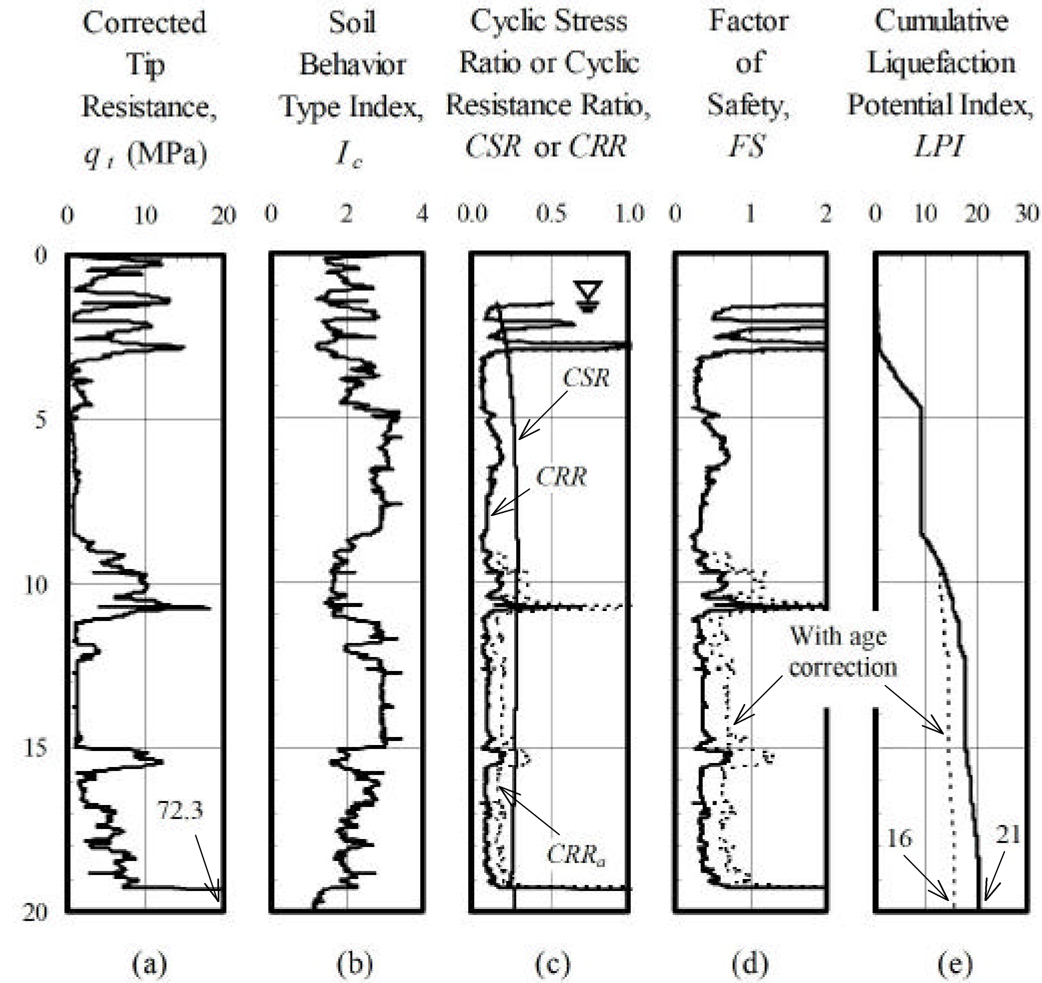

Figure 5. Calculation of *LPI* for CPT site number 26 based on M_w = 7.1 and a_{max} = 0.3 g.

Summarized in Table 4 and plotted in Figure 6(a) are median, mean, and ± 1 standard deviation of *LPI* values calculated for the four site geology categories. The mean and ± 1 standard deviation values are determined assuming a log-normal distribution and using Rankit analysis, as suggested by Balon and Andrus (2006). It can be seen in the table and the figure that mean and median values for each category are close.

Median *LPI* values for the four site geology categories (i.e., Qht, Qht/Qhes, Qhes, and Qws) are 6, 10, 16 and 17, respectively. According to the criteria by Iwasaki et al. (1982), a *LPI* value around 6 suggests not likely to moderate liquefaction potential, which agrees with observed behavior for Qht sites. A value of 10 suggests moderate liquefaction potential, and seems reasonable for Qht/Qhes sites. Median LPI values of 16 and 17 indicate moderate to severe liquefaction potential. A prediction of severe liquefaction agrees with observed behavior for Qhes sites, but is too high for Qws sites. Based on these findings, there appears to be no need to change a_{max} or apply an age correction factor to the Qht and Qhes layers. On the other hand, it seems appropriate to apply an age correction to the Wando Formation to obtain a median *LPI* value closer to 5 for Qws sites and agree with observed field behavior.

With Age Correction

By setting a target *LPI* value of 5 for Qws sites, and assuming K_{a2} = 1.0 for all younger units, an approximate K_{a2} value can be obtained for the Wando Formation. The K_{a2} value that provides a median *LPI* value of 5 for Qws sites is 1.8. The dashed lines plotted in Figures 5(c), 5(d) and 5(e) represent the *CRR*, *FS* and *LPI*, respectively, calculated assuming this age correction. Summarized in Table 4 and plotted in Figure 6(b) are the statistics of *LPI* based on K_{a2} = 1.8 for the Wando Formation and K_{a2} = 1.0 for all younger units.

Median *LPI* values based on this age correction for the four site categories are 5, 7, 13 and 5, respectively. It is interesting to note that the *LPI* values for all four categories are lower than values determined with on no age correction, because the Wando Formation underlies many of the investigation sites in the top 20 m. *LPI* values of 5 for Qht, 7 for Qht/Qhes and 13 for Qhes sites are still reasonable for the observed field behavior. Thus, a K_{a2} value of 1.8 is appropriate for Wando Formation and agrees well with the middle range value of 1.9 suggested by Arango et al. (2000) for 100,000-year-old deposits.

Table 4. Statistics of *LPI* with and without age corrections

Site geology category	Number of CPTs	Without age correction			With age correction		
		Median *LPI*	Mean *LPI*	±1 Standard deviation	Median *LPI*	Mean *LPI*	±1 Standard deviation
Qht	15	6	6	2-10	5	6	2-9
Qht/Qhes	5	10	11	6-16	7	8	6-10
Qhes	8	16	17	10-24	13	13	6-19
Qws	16	17	18	12-24	5	5	2-8

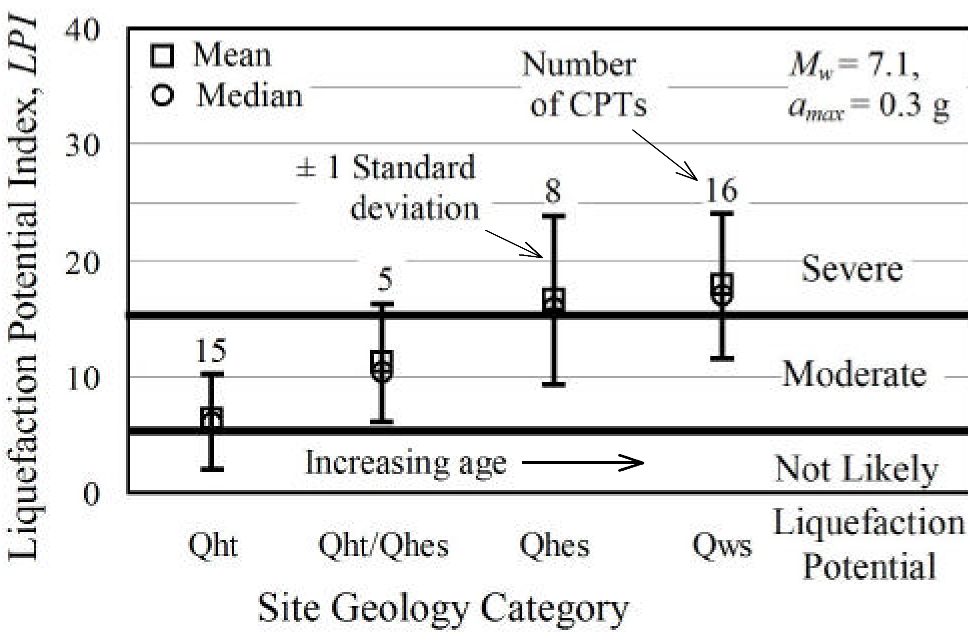

(a)

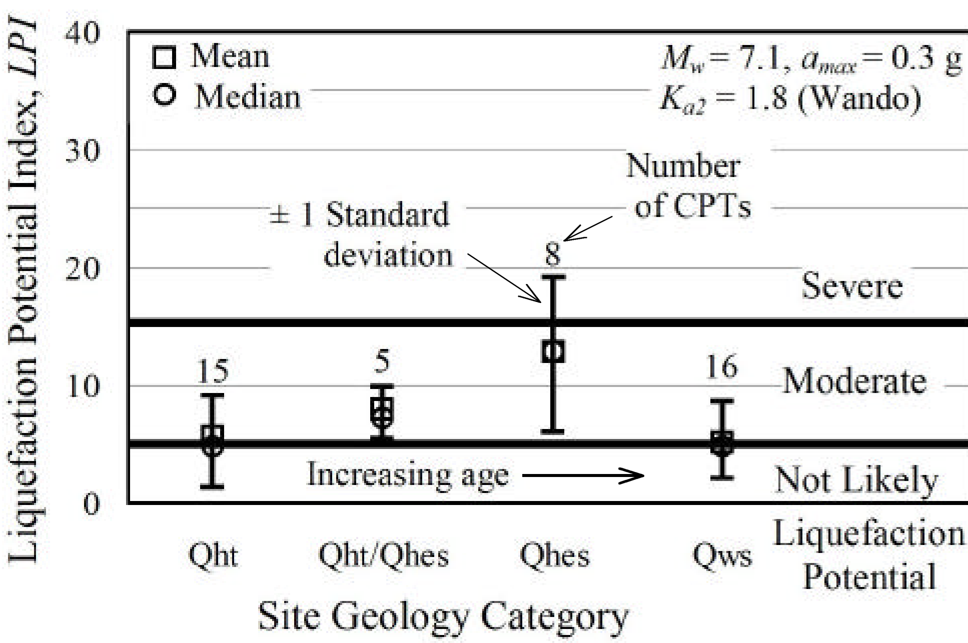

(b)

Figure 6. Statistics of LPI values grouped by geology (a) without age correction, and (b) with age correction applied to the Wando Formation.

Uncertainty

To try to quantify the uncertainty of the back-calculated K_{a2} value of 1.8, the calculations are repeated using recent published estimates of the 1886 earthquake shaking parameters. As noted earlier, the estimates of earthquake magnitude range from as low as 6.6 (Bakun and Hopper, 2004) to as high as 7.6 (Frankel et al. 2002). Estimates of a_{max} are limited by the uncertainties associated with the 1886 source characteristics and the regional attenuation relationship. Chapman et al. (2006) used a point-source stochastic model and reasonable input parameters to obtain mean a_{max} values ranging from 0.2 g for M_w = 6.1 to 0.48 g for M_w = 7.6. Using their implied M_w-a_{max} relationship for Charleston and assuming calculated median *LPI* values should be within $\pm$20 % of target *LPI* values of 5, 15 and 5 for Qht, Qhes and Qws, respectively, K_{a2} values as low as 1.0 (no age correction) to over 3.0 are obtained. This range for K_{a2} exceeds the range suggested by Arango et al. (2000) for 100,000-year-old deposits. Thus, the great uncertainty associated with the 1886 ground shaking level makes it difficult to constrain K_{a2} within reasonable limits.

If K_{a2} values of 1.3 to 2.5 are assumed as a reasonable range for 100,000-year-old soils based on the relationship proposed by Arango et al. (2000), the magnitude of 1886 earthquake can be constrained to a much narrower range than previously suggested. Assuming these K_{a2} values and the M_w-a_{max} relationship suggested by Chapman et al. (2006), the minimum shaking level of M_w = 7.0 with a_{max} = 0.27 g and the maximum shaking level of M_w = 7.4 with a_{max} = 0.40 g are required to keep the median *LPI* values of each category within ± 20 % of the target values. This estimated range for likely earthquake shaking levels supports the approximate middle range values of M_w = 7.1 and a_{max} = 0.3 g initially assumed for the *LPI* calculations.

1886 LIQUEFACTION POTENTIAL MAP

The *LPI* values based on M_w = 7.1, a_{max} = 0.3 g and K_{a2} = 1.8 for the Wando Formation are adopted to produce the 1886 liquefaction potential map of Charleston peninsula and Drum Island shown in Figure 7. The map is divided in to two general liquefaction potential zones: 1) moderate to severe, and 2) not-likely to moderate. The two zones are identified based on the *LPI* values and the field behavior cases (see Figure 2).

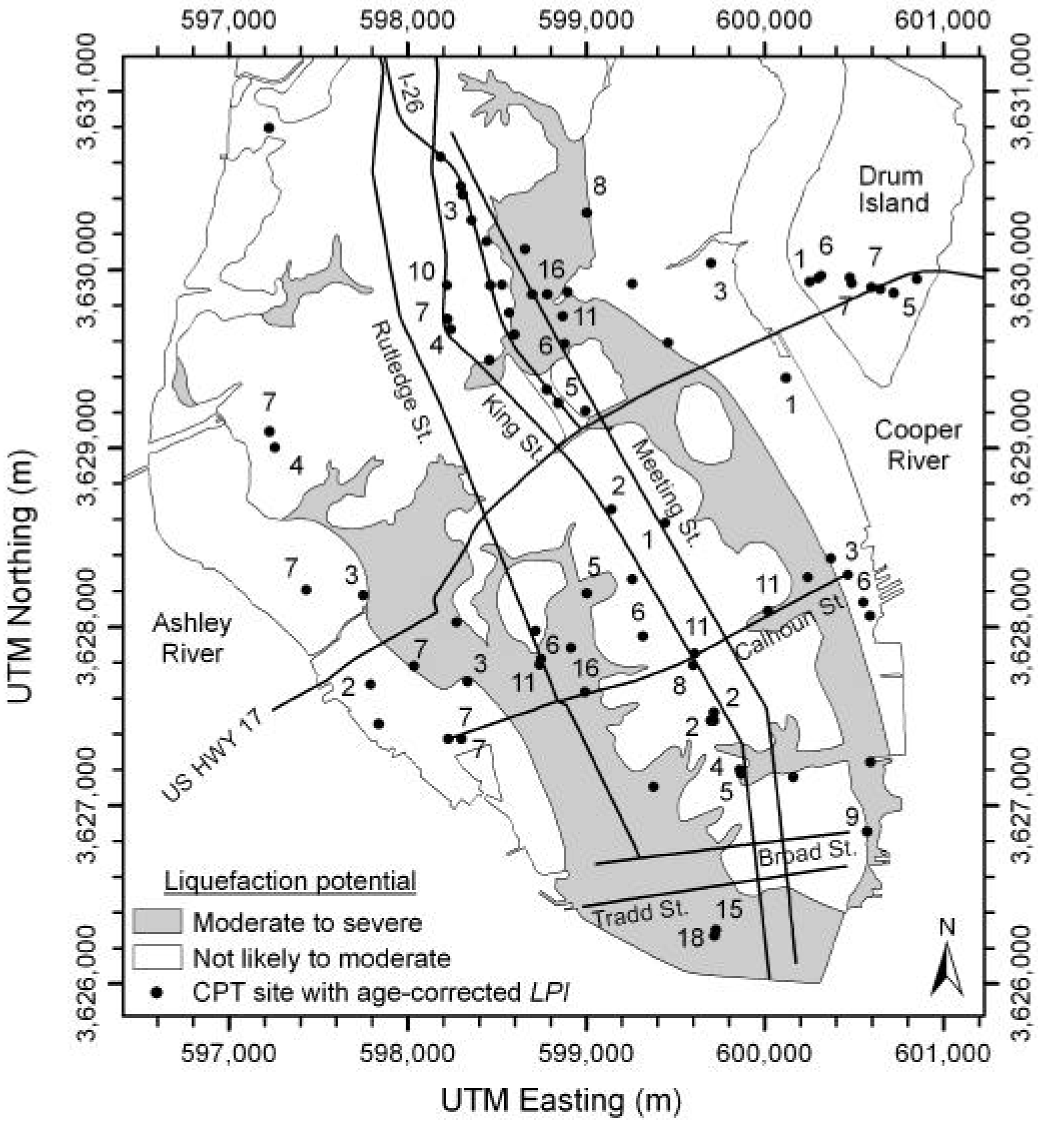

Figure 7. Liquefaction potential map of Charleston peninsula and Drum Island based on1886 field performance data and age-corrected *LPI*.

The zone of moderate to severe liquefaction potential covers the Qhes and af/Qhes surficial deposits. In this zone, the ±1 standard deviation range of *LPI* is 6-19. For the inner boundary, contacts between Qhes and Qws are taken directly from the surficial geology map. The outer boundary is drawn conservatively to include all sites in the Qhes category and sites where Qhes is believed to underlie af or Qht. The four values of *LPI* ≥ 15 indicate severe liquefaction potential at some locations in this zone. This assessment is supported by the fact that all but one of the 1886 liquefaction cases listed in Table 1 are located in the zone of moderate to severe liquefaction potential.

The zone of unlikely to moderate liquefaction potential includes the areas of Qws and Qht deposits. The ±1 standard deviation range of *LPI* is 2-8 in this zone. The two *LPI* values ≥ 10 indicate that areas of moderate liquefaction potential are possible in Qws deposits, and may explain the one case of settlement reported in this zone (site number 14 in Table 1). The assessment of not likely to moderate liquefaction potential is further supported by the cases of no ground failure (see Table 2).

The map presented in Figure 7 provides a useful tool for planners working to mitigate damage in Charleston during future earthquakes. Buildings and utilities within the moderate to severe zone are vulnerable to liquefaction-induced settlement, ground movements, and flow of soil and water into basements. Buildings and buried utilities that straddle the two zones are particularly vulnerable to failure caused by lateral ground movements. When using the map, caution should be applied in areas of af because this material has a random consistency and hides the underlying natural sediments. The map does not replace site-specific liquefaction potential and ground failure evaluations for final project design.

CONCLUSIONS

The liquefaction potential of soil deposits on Charleston peninsula is investigated through analysis of CPT profiles and review of cases of liquefaction and ground deformation. It is found that nearly all cases of liquefaction and ground deformation can be related to the Qhes deposits. Only one case of ground deformation (i.e., settlement of the St. Michael's Church tower) can be related to the Qws deposits. Thus, very few instances of liquefaction occurred in the Qws deposits on the peninsula in 1886. This conclusion is further supported by several cases of no ground deformation associated with Qws. Based on these findings, target median

LPI values of 5, 10, 15 and 5 are assumed for geologic units Qht, Qht/Qhes, Qhes and Qws, respectively.

To compute *LPI* from the CPT profiles, middle range values of 7.1 and 0.3 g for the 1886 earthquake magnitude and peak ground surface acceleration, respectively, are initially assumed. A comparison of target and computed median *LPI* values suggests an age correction factor of 1.8 to increase cyclic resistance ratios in Qws is needed. This age correction factor agrees well with the middle range value suggested by Arango et al. (2000) for 100,000-year-old deposits. No age correction appears to be needed for the younger deposits.

The great uncertainty associated with the 1886 ground shaking level makes it impossible to reasonably quantify the uncertainty of the back-calculated age correction factor for Qws. On the other hand, assuming age correction factors of 1.3 and 2.5 as lower and upper limits based on the work of Arango et al. (2000), the magnitude of 1886 earthquake can be constrained to 7.0-7.4, if computed median *LPIs* are restricted to be within $\pm$20 % of the target values.

Using the computed *LPI* values, a geologic map and the observed field behavior information, a new liquefaction potential map of Charleston peninsula is developed. The map is divided into two zones. The zone of moderate to severe liquefaction potential includes the Qhes deposits. The zone of unlikely to moderate liquefaction potential includes the Qht and Qws deposits. This new map can be a useful tool for planners, engineers, and scientists working to mitigate future earthquake damage in Charleston. Site-specific liquefaction potential and ground failure evaluations should be conducted for final project design, however.

REFERENCES

Arango, I., Lewis, M. R., and Kramer, C. (2000). "Updated liquefaction potential analysis eliminates foundation retrofitting of two critical structures," *Soil Dynamics and Earthquake Engineering,* 20, 17-25.

Andrus, R. D., Fairbanks, C. D., Zhang, J., Camp, W. M. III, Casey, T. J., Cleary, T. J., and Wright, W. B. (2006). "Shear-wave velocity and seismic response of near-surface sediments in Charleston, South Carolina," *Bulletin of the Seismological Society of America,* 96(5), 1897-1914.

Bakun, W. H., and Hopper, M. G. (2004). "Magnitudes and locations of the 1811-1812 New Madrid, Missouri, and the 1886 Charleston, South Carolina, earthquakes," *Bulletin of the Seismological Society of America*, 94, 64-75.

Balon, D. R., and Andrus, R. D. (2006). "Liquefaction potential index of soils in Charleston, South Carolina based on the 1886 earthquake," *Proc. of the 8th U.S. National Conference on Earthquake Engineering*, April 18-26, San Francisco, CA.

Bollinger, G. A. (1977). "Reinterpretation of the intensity data for the 1886 Charleston, South Carolina, earthquake," *Studies Related to the Charleston, South Carolina, Earthquake of 1886: A Preliminary Report*, D. W. Rankin (Editor), *USGS Professional Paper 1028*, U.S. Geological Survey, 17-32.

Boulanger, R. W., and Idriss, I. M. (2006). "Liquefaction susceptibility criteria for silts and clays," *Journal of Geotechnical and Geoenvironmental Engineering*, 132(11), 1413-1426.

Bray, J. D., and Sancio, R. B., (2006). "Assessment of the liquefaction susceptibility of fine-grained soils," *Journal of Geotechnical and Geoenvironmental Engineering*, 132(9), 1165-1177.

Chapman M. C., Martin, J. R., Olgun, C. G., and Beale, J. N. (2006). "Site-response models for Charleston, South Carolina and vicinity developed from shallow geotechnical investigations," *Bulletin of the Seismological Society of America*, 96(2), 467-489.

Côté, R. N. (2006). *City of Heroes: The Great Charleston Earthquake* of 1886, Corinthian Books, Mount Pleasant, SC, 542 p.

Dutton, C. E. (1889). "The Charleston earthquake of August 31, 1886," *USGS Ninth Annual Report 1887-1888*, U.S. Geological Survey, Washington, D.C., 203-528.

Elton, D. J., and Hadj-Hamou, T. (1990). "Liquefaction potential map for Charleston, South Carolina," *Journal of the Geotechnical Engineering Division*, 116(2), 244-265.

Elton, D. J., and Marciano, E. A. (1990). "Ground acceleration near St. Michael's Church during the 1886 Charleston, SC, earthquake," *Earthquake Spectra*, 6(1), 81-103.

Fairbanks, C. D. (2006). "Shear-wave velocity model of near-surface sediments, site response, and building damage: 1886 Charleston, South Carolina earthquake," *Ph.D. Dissertation*, Clemson University, Clemson, SC.

Fairbanks, C. D., Andrus, R. D., Zhang, J., Camp, W. M., Casey, T. J., and Clearly, T. J. (2004). "Electronic files of shear-wave velocity and cone penetration test measurements from the Charleston quadrangle, South Carolina," Data report to the U.S. Geological Survey, Award Number 03HQGR0046, Civil Engineering Dept., Clemson University, Clemson, SC.

Frankel, A. D., Petersen, M. D., Mueller, C. S., Haller, K. M., Wheeler, R. L., Leyendecker, E. V., Wesson, R. L., Harmsen, S. C., Cramer, C. H., Perkins, D. M., and Rukstales K. S. (2002). "Documentation for the 2002 update of the national seismic hazards maps," *USGS Open-File Report 02-420*, U.S. Geological Survey, Denver, CO.

Gilstrap, S. D. (1998). "CPT based liquefaction resistance analyses evaluated using case histories," *M.S. Thesis*, Brigham Young University, Provo, UT.

Holzer, T. L., Bennett, M. J., Noce, T. E., Padovani, A. C., and Tinsley, J. C. III (2006). "Liquefaction hazard mapping with LPI in the greater Oakland, California, area," *Earthquake Spectra*, 22(3), 693-708.

Hynes, M. E., and Olsen, R. (1999). "Influence of confining stress on liquefaction resistance," *Proc., Int. Workshop on the Phys. and Mech. of Liquefaction,* Balkema, Rotterdam, The Netherlands, 145-152.

Idriss, I. M., and Boulanger, R. W. (2003). "Relating K_α and K_σ to SPT blow count and to CPT tip resistance for use in evaluating liquefaction potential," *Proc., 20th Annual Conference of Association of State Dam Safety Officials,* ASDSO, Lexington, KY.

Iwasaki, T., Tatsuoka, F., Tokida, K.-I., and Yasuda, S. (1978). "A practical method for assessing soil liquefaction potential based on case studies at various sites in Japan," *Proc., 2nd International Conference on Microzonation*, San Francisco, CA, 885-896.

Iwasaki, T., Tokida, K., Tatsuoka, F., Watanabe, S., Yasuda, S. and Sato, H. (1982). Microzonation for soil liquefaction potential using simplified methods, *Proc., 3rd International Earthquake Microzonation Conference*, Seattle, WA, 1319-1330.

Leon, E., Gassman, S. L. and Talwani, P. (2006). "Accounting for soil aging when assessing liquefaction potential," *Journal of Geotech. and Geoenvironmental Eng.*, 132(3), 363-377.

Li, D. K., and Juang, C. H. (2006). "Mapping liquefaction-induced ground failure potential in Charleston quadrangle, South Carolina," *Proc. of the 8th U.S. National Conference on Earthquake Engineering*, April 18-26, San Francisco, CA.

Li, D. K., Juang. C. H., Andrus, R. D. and Camp. W. M. (2007). "Index properties-based criteria for liquefaction susceptibility of clayey soils: a critical assessment," *Journal of Geotechnical and Geoenvironmental Engineering,* 133(1), 110-115

Liao. S. C. and Whitman, R. V. (1986). "Overburden correction factors for SPT in sand," *Journal of Geotechnical Engineering* , 112(3), 373-377

Lunne. T., Robertson, P., and Powel, J. (1997). *Cone Penetration Testing in Geotechnical Practice*, Thomson, Florence, KY

Mohanan, N. P., Fairbanks, C. D., Andrus, R. D., Camp, W. M., Clearly, T. J., Casey, T. J., and William B. Wright (2006). "Electronic files of shear wave velocity and cone penetration test measurements from the greater Charleston area, South Carolina," Data report to the U.S. Geological Survey, Award Number 05HQGR0037, Civil Engineering Dept., Clemson University, Clemson, SC.

Peters, K. E., and Herrman, R. B., Editors (1986). "First-hand observations of the Charleston Earthquake of August 31, 1886, and other earthquake materials: reports of W J McGee, Earle Sloan, Gabriel E. Manigault, Simon Newcomb, and others," *South Carolina Geological Survey Bulletin 41*, Columbia, SC, 116 p.

Robertson, P. K., and Wride, C. E. (1998). "Evaluating cyclic liquefaction potential using the cone penetration test," *Canadian Geotechnical Journal*, 35(3), 442-459.

Robinson, A., and Talwani, P. (1983). "Building damage at Charleston, South Carolina, associated with the 1886 earthquake," *Bulletin of the Seismological Society of America,* 73(2), 633-652.

Seed, H. B., and Idriss, I. M. (1971). "Simplified procedure for evaluating soil liquefaction potential," *Journal of the Geotechnical Engineering Division*, 97(9), 1249-1273.

Seed, H. B., and Idriss, I. M. (1982). "Ground motions and soil liquefaction during earthquakes," Earthquake Engineering Research Institute Monograph, Oakland, CA.

Silva, W., Wang, I., Siegel, T., Gregor, N., Darragh, R., and Lee R. (2003). "Ground motion and liquefaction simulation of the 1886 Charleston, South Carolina, earthquake," *Bulletin of the Seismological Society of America*, 93(6), 2717-2736.

Toprak, S., and Holzer, T. L. (2003). "Liquefaction potential index: field assessment," *Journal of Geotechnical and Geoenvironmental Engineering,* 129(4), 315-322.

Weems, R. E., and Lemon, E. M. Jr., (1993). "Geology of the Cainhoy, Charleston, Fort Moultrie, and North Charleston Quadrangles, Charleston and Berkley Counties, South Carolina," *USGS Misc. Investigation Map I-1935, scale 1:24,000*, Department of the Interior, U.S. Geological Survey, Reston, VA.

Weems R. E., Lemon, E. M. Jr., and Chirico P. (1997). "Digital geology and topography of the Chaleston quadrangle, Charleston and Berkeley counties, South Carolina," *USGS Open-File Report 00-0484,* U.S. Geological Survey, Reston, VA.

Wong, I., Bouabid, J., Graf, W., Huyck, C., Porush, A., Silva, W., Siegel, T., Bureau, G., Eguchi, R., and Knight J. (2005). "Potential losses in a repeat of the 1886 Charleston, South Carolina, earthquake," *Earthquake Spectra*, 21(4), 1157-1184.

Youd, T.L., and Hoose, S.N. (1977). "Liquefaction susceptibility and geologic setting," Proc. 6^{th} World Conference on Earthquake Engineering, New Delhi, India, Vol. 6, 37-42

Youd, T.L., and Perkins, D. M. (1978). "Mapping of liquefaction-induced ground failure potential," *Journal of Geotechnical Engineering Division*, ASCE, 104(4), 433-446.

Youd, T. L., Idriss, I. M., Andrus, R. D., Arango, I., Castro, G., Christian, J. T., Dobry, R., Finn, W. D. L., Harder, L. F. Jr., Hynes, M. E., Ishihara, K., Koester, J. P., Liao, S. S. C., Marcuson,

W. F. III, Martin, G. R., Mitchell, J. K., Moriwaki, Y., Power, M. S., Robertson, P. K., Seed, R. B., and Stokoe, K. H. II, (2001). "Liquefaction resistance of soils: summary report from the 1996 NCEER and 1998 NCEER/NSF workshops on evaluation of liquefaction resistance of soils," *Journal of Geotechnical and Geoenvironmental Engineering*, 127(10), 817-833.

Zhang, G., Robertson, P. K., and Brachman, R. W. I. (2002). "Estimating liquefaction-induced ground settlements from CPT for level ground," *Canadian Geotech. Journal*, 39(5), 1168-1180.

APPENDIX

COMPACT DISK WITH ELECTRONIC COPY OF THE FINAL REPORT